



HAL
open science

Full quantum determination of the quasiequilibrium constant involved in the formation of ozone

G. Guillon, P. Honvault

► **To cite this version:**

G. Guillon, P. Honvault. Full quantum determination of the quasiequilibrium constant involved in the formation of ozone. *Physical Review Research*, 2024, 6 (4), pp.043181. 10.1103/PhysRevResearch.6.043181 . hal-04812016

HAL Id: hal-04812016

<https://hal.science/hal-04812016v1>

Submitted on 8 Dec 2024


HAL is a multi-disciplinary open access archive for the deposit and dissemination of scientific research documents, whether they are published or not. The documents may come from teaching and research institutions in France or abroad, or from public or private research centers.

L'archive ouverte pluridisciplinaire **HAL**, est destinée au dépôt et à la diffusion de documents scientifiques de niveau recherche, publiés ou non, émanant des établissements d'enseignement et de recherche français ou étrangers, des laboratoires publics ou privés.



Distributed under a Creative Commons Attribution 4.0 International License

Full quantum determination of the quasiequilibrium constant involved in the formation of ozone

G. Guillon^{*} and P. Honvault[†]*Laboratoire ICB, CNRS and Université de Bourgogne, 21078 Dijon, France* (Received 27 May 2024; revised 15 August 2024; accepted 5 November 2024; published 21 November 2024)

Forty years ago, measurements of enrichments in ^{18}O in stratospheric ozone O_3 revealed a value significantly greater than statistically expected and roughly equal in heavy isotopes ^{17}O and ^{18}O . Despite numerous experimental and theoretical studies, this mass-independent fractionation (MIF) still remains unexplained. However, it is now accepted that its origin comes from isotopic effects found in the recombination reaction $\text{O} + \text{O}_2 + M \rightarrow \text{O}_3 + M$ where M is a stabilizer, even if the theoretical origin of the isotope effects found in this reaction is still not known. Here we study the first of the two steps involved in this reaction, namely, the rapid quasiequilibrium $\text{O} + \text{O}_2 \rightleftharpoons \text{O}_3^*$ process where O_3^* is metastable ozone. The quasiequilibrium constant for this process is obtained from a full quantum dynamical approach. These high-level calculations yield the most accurate value of this quantity to date for $^{48}\text{O}_3$ and $^{50}\text{O}_3$. These reference results constitute a crucial stage for a better understanding of the ozone formation reaction, and could therefore help to unravel the mystery of MIF.

DOI: [10.1103/PhysRevResearch.6.043181](https://doi.org/10.1103/PhysRevResearch.6.043181)

I. INTRODUCTION

Ozone, O_3 , is a critical molecule for the survival of humanity on Earth through its presence in the stratosphere by protecting us from the dangerous ultraviolet rays. However, in the troposphere it is considered as an air pollutant that can cause health problems. In the atmosphere O_3 is mainly formed by three identical atoms of oxygen 16, i.e., $^{16}\text{O}^{16}\text{O}^{16}\text{O}$. We know that the oxygen atom has three stable isotopes with terrestrial abundances of 99.759% ^{16}O , 0.037% ^{17}O , and 0.204% ^{18}O . The rules of isotope thermodynamic fractionation suggest that isotope enrichments measured from the concentration ratios $^{18}\text{O}^{16}\text{O}^{16}\text{O} / ^{16}\text{O}^{16}\text{O}^{16}\text{O}$ and $^{17}\text{O}^{16}\text{O}^{16}\text{O} / ^{16}\text{O}^{16}\text{O}^{16}\text{O}$ should be statistically correlated with the relative mass difference of the isotopes, which is called the isotope-dependent mass effect [1].

However, in 1981, measurements of ^{18}O in stratospheric ozone [2] revealed a significant enrichment in heavy isotopologues. This unusual enrichment was then reproduced in laboratory measurements [3], which confirmed the trends observed previously, with, notably, a roughly equal enrichment in monosubstituted heavy isotopologues $^{17}\text{O}^{16}\text{O}^{16}\text{O}$ ($^{49}\text{O}_3$) and $^{18}\text{O}^{16}\text{O}^{16}\text{O}$ ($^{50}\text{O}_3$). These experiments also provided enrichment values for all possible (polysubstituted) isotopologues in highly exotic oxygen mixtures. This isotope anomaly is commonly called mass-independent fractionation (MIF) due to its deviation from the mass-dependent fraction-

ation line. The ozone MIF is photochemically transferred to atmospheric oxygen bearing species such as CO_2 , O_2 , sulfates, and nitrates, and therefore plays a major role in various fields such as atmospheric chemistry, geochemistry, cosmochemistry, and climate research [1,4].

Since the MIF discovery, a large number of experimental and theoretical studies have been devoted to understand this puzzling phenomenon [5–15]. However, to date, no first principles explanation has been found and the origin of the MIF remains an unsolved mystery. It is now well established that this anomaly is related to the significant kinetic isotope effects [1,4] observed [7–10] in one of the process involved in the well-known Chapman cycle, the so-called three-body recombination reaction



with M being a buffer gas (most likely N_2/O_2 molecules or Ar atoms). However, the theoretical origin of the isotope effects found in reaction (1) is still not known. The origin of MIF comes from isotopic effects found experimentally in the recombination reaction (1) because this is the reaction which forms stable ozone in the atmosphere, with different recombination rates k^{rec} , depending on specific ozone isotopologues obtained in the end. However, these different values of k^{rec} have just been measured, and the origin of these differences is not explained to date from first principles. This is why the ozone MIF remains a mystery because it is still unexplained from a theoretical viewpoint.

Knowing more about reaction (1) would add a stone to the understanding of the ozone MIF. It was found that the specific formation rates, k^{rec} , of O_3 by this process are smaller for symmetrical isotopomers of ozone (e.g., $^{16}\text{O}^{18}\text{O}^{16}\text{O}$) than those for asymmetrical isotopomers (e.g., $^{18}\text{O}^{16}\text{O}^{16}\text{O}$) [7–10]. Janssen *et al.* [9] found these quantities in a rough correlation with the differences in the quantum mechanical (QM) zero-point energy of the various diatomic O_2 reactants. No

*Contact author: gregoire.guillon@u-bourgogne.fr†Contact author: pascal.honvault@univ-fcomte.fr

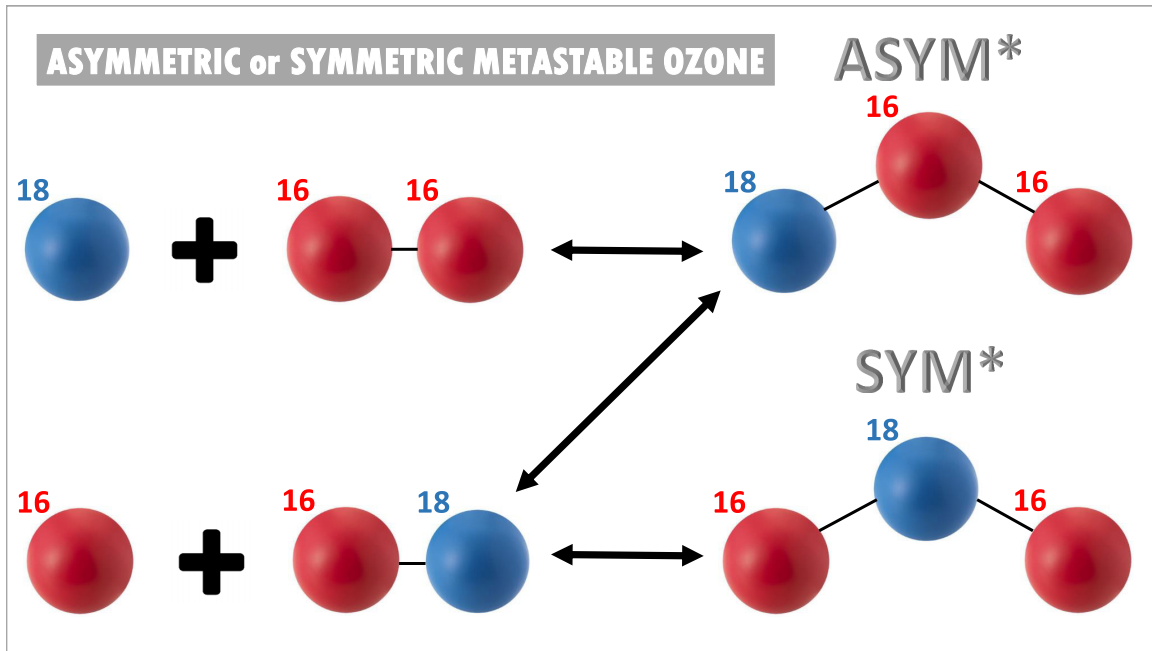
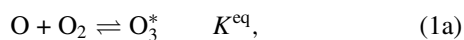


FIG. 1. Quasiequilibrium processes involving symmetric or asymmetric metastable ozone. The upper panel shows the $^{18}\text{O}^{16}\text{O}^{16}\text{O}^*$ asymmetric metastable ozone formed from the $^{18}\text{O} + ^{16}\text{O}^{16}\text{O}$ collision and that dissociates towards the same species or towards $^{16}\text{O} + ^{16}\text{O}^{18}\text{O}$. The lower panel shows the $^{16}\text{O}^{18}\text{O}^{16}\text{O}^*$ symmetric metastable ozone formed from the $^{16}\text{O} + ^{16}\text{O}^{18}\text{O}$ collision and that dissociates towards the same species.

direct full quantum calculation of k^{rec} has ever been performed to date due to the great difficulty in describing this process quantumly. Only a recent classical trajectory study [15] has been reported giving the k^{rec} value for the formation of $^{16}\text{O}^{16}\text{O}^{16}\text{O}$. At atmospheric pressures and temperatures, the Lindemann mechanism is believed to be the dominant process for ozone formation, although another mechanism may also play an important role at high pressures and low temperatures [15–17]. In the Lindemann mechanism, reaction (1) can be decomposed into two main steps:



with M carrying out the excess energy to yield stable ozone O_3 , and with O_3^* the metastable ozone, i.e., a long-lived resonant scattering state above the dissociation energy of the electronic ground state of ozone. Several attempts to explain the measured isotope effects [7–10] found in reaction (1) were based on arguments of symmetry [6,13,18–22], which could result in different lifetimes of the O_3^* metastable species. The association/dissociation reaction (1a) is characterized by the quasiequilibrium constant K^{eq} (see Appendix A for a precise definition), while the deactivation process (1b) is characterized by the stabilization constant k^{stab} . In the low-pressure regime, when step (1a) is two to three orders of magnitude faster than (1b), we can write k^{rec} as the product $K^{\text{eq}}k^{\text{stab}}$. Knowledge of K^{eq} and k^{stab} , therefore, allows determination of the rate of ozone formation by reaction (1). The K^{eq} and k^{stab} quantities were determined indirectly by experiments [23–25] in the 1960s and no measurements were published since this pioneering work. From the theoretical point of view, they were computed using approximate methods only, classical

treatment [26], method mixing classical and quantum mechanics [27,28], and various quantum models [29–33]. A fully QM calculation of K^{eq} and k^{stab} has never been accomplished to date.

The origin of ozone MIF is an effect present in either step (1a), or step (1b), or both [4,33,34]. It is therefore necessary to correctly describe these two stages, that is to say in a rigorous quantum way. In this article, we report calculations of the K^{eq} values for the following processes (1a): $^{16}\text{O} + ^{16}\text{O}^{16}\text{O} \rightleftharpoons ^{16}\text{O}^{16}\text{O}^{16}\text{O}^*$, $^{18}\text{O} + ^{16}\text{O}^{16}\text{O} \rightleftharpoons ^{16}\text{O}^{18}\text{O}^{16}\text{O}^*$ and $^{16}\text{O} + ^{16}\text{O}^{18}\text{O} \rightleftharpoons ^{18}\text{O}^{16}\text{O}^{16}\text{O}^*$ or $^{16}\text{O}^{18}\text{O}^{16}\text{O}^*$, as shown in Fig. 1, by using a pure QM formalism. They will be abbreviated in the following as 6 + 66, 8 + 66, and 6 + 68. To the best of our knowledge, this treatment is the most accurate to date to calculate K^{eq} and the present numerical results may serve as reference values. They also provide new perspectives on the ozone MIF problem. In the Earth’s atmosphere and particularly in the stratosphere, the most abundant ozone is of course $^{48}\text{O}_3$ (three ^{16}O atoms, 99.3%) followed by $^{50}\text{O}_3$ (one ^{18}O atom and two ^{16}O atoms, 0.6%), ozone enriched in ^{17}O ($^{49}\text{O}_3$) being by far the one with the lowest abundance (0.1%). Other isotopic variants like $^{16}\text{O}^{17}\text{O}^{18}\text{O}$ or the doubly substituted species (as, for instance, $^{18}\text{O}^{18}\text{O}^{16}\text{O}$) are negligible. This is why we focused here on $^{48}\text{O}_3$ and $^{50}\text{O}_3$.

II. THEORY

All the QM calculations were performed using our own code using a time-independent QM approach based on hyperspherical coordinates [35,36]. We employed the O_3 potential energy surface (PES) calculated using the multireference configuration interaction (MRCI) method [37]. This *ab initio* PES has proved to be the most accurate for spectroscopic purposes

[38,39] and for scattering calculations of the $O + O_2$ exchange reaction [40]. This code allows the computation of the scattering S -matrix, from which state-to-state reaction probabilities, cross sections and rate constants for atom-exchange triatomic reactions, such as $A + BC \rightarrow AB + C$, can be derived. Details of the quantum formalism for the study of such reactions can be found in Ref. [36]. Our QM code, initially developed to perform accurate calculations of cross sections and rate constants for exchange reactions, is robust and has previously proved successful in describing dynamics of atom-diatom reactions [40–43]. To compute the quasiequilibrium constant K^{eq} of the (1a) process, we used the Smith Q -matrix quantum formalism [44] (see Appendices B and C for the necessary details) that is based on the scattering S -matrix. We recently implemented this formalism in our code to calculate the lifetimes of some metastable states of O_3^* [45,46]. In other words, the Q -matrix elements as a function of total energy E and at a given total angular momentum J are directly related to the S -matrix elements for the same E and J . As the S -matrix, the Q -matrix is an output quantity containing maximal information on the dynamics of the collisional (reactive, inelastic, or elastic) event. Once the Q -matrix is determined, its trace, $\text{Tr } Q$, can be calculated and then K^{eq} can be derived from it. QM calculations were performed for a relatively thin energy grid (with a constant step size of 6×10^{-5} eV) for a total energy E up to 0.5 eV, and for J values from 0 to 114 included in the close-coupled equations. This energy grid was found sufficient for an accurate estimation of integrals over density of resonance states, yielding rovibrational partition functions for O_3^* metastable complex. This was checked from various trials of numerical integration and alternative summation methods. The step size was chosen to keep a manageable number of energy data, and does not come from a limitation of the algorithm providing the Q -matrix itself [46]. We carefully checked that the values of all the parameters employed in the QM calculations were sufficient to obtain convergence of the K^{eq} values up to a temperature of 400 K.

More details on the method used here and the present quantum calculations can be found in Appendices A–C. We present here both complete and accurate results to date concerning the quasiequilibrium preliminary step (1a) for the formation of ozone through reaction (1).

III. RESULTS AND DISCUSSION

As clearly seen in Fig. 2, quasiequilibrium constants for the three types of processes, $6 + 66$, $8 + 66$, and $6 + 68$, are all decreasing with temperature in a monotonic fashion, all the way from 100 to 400 K. The constant for the process involving only ^{16}O atoms, K_{6+66}^{eq} , remains below the value of the $10^{-22} \text{ cm}^3 \text{ molecule}^{-1}$ for all considered temperatures. On the other hand, one of the two constants for the equilibrium in presence of the heavy ^{18}O atom, with reactants $8 + 66$, K_{8+66}^{eq} , is exceeding twice this value at the lowest temperatures (close to 100 K). We clearly attribute this result to the much higher density of resonance states of substituted ozone complex 866^* compared to the 666^* complex, as can be checked by comparing of Figs. 4 and 5. In these figures, the two plots reveal a much higher

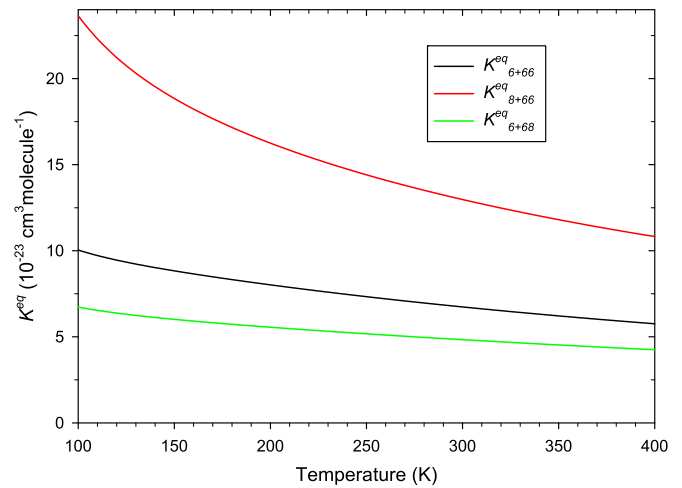


FIG. 2. Quasiequilibrium constant as a function of temperature. Results for the reference $6 + 66$ process (black line), as well as for the two processes $8 + 66$ (red line), and $6 + 68$ (green line) involving one heavy oxygen isotope.

background density of resonance states for $^{50}O_3^*$ than for $^{48}O_3^*$, for which peaks are sparse, resonances being isolated and nonoverlapping. The $^{50}O_3^*$ complex also exhibits much longer lifetimes, especially for high values of the total angular momentum J .

The density of states of 866^* is about three times larger than that of 666^* based on the ratio of the energy-integrals of the trace of the Smith matrix. This can be explained by the greater symmetry of 666^* leading to a severe restriction of the number of metastable states accessible for 666^* . This means that in an oxygen mixture with a nonnegligible proportion of ^{18}O , especially at low temperatures, the concentration of $^{50}O_3^*$ complexes tends to become much higher than expected on the grounds of purely statistical mass-dependent fractionation rules. This statement remains true up to 400 K,

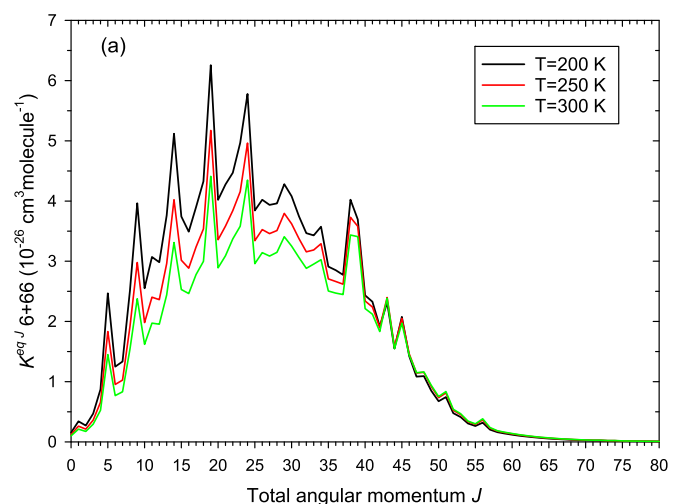


FIG. 3. Quasiequilibrium constant J components for the $6 + 66$ reference process as a function of the total angular momentum J for temperatures $T = 200, 250, \text{ and } 300$ K.

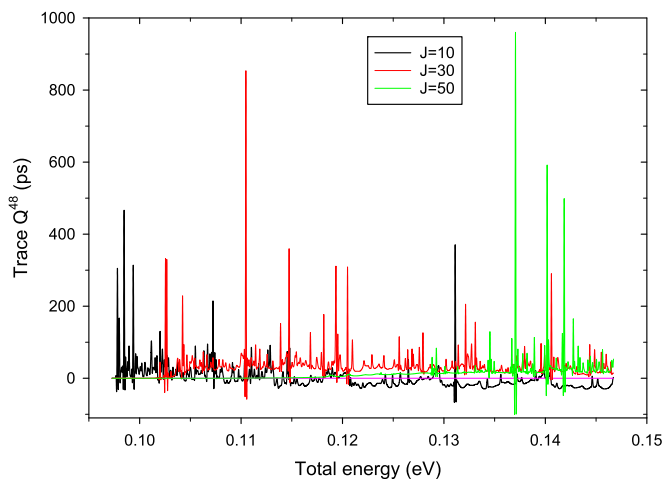


FIG. 4. Global lifetimes of $^{48}\text{O}_3^*$ complex, $\text{Tr } \mathbf{Q}_{48}^J(E)$, as a function of total energy E , for $J = 10, 30$, and 50 .

as the ratio between the two above-mentioned equilibrium constants, $K_{8+66}^{\text{eq}}/K_{6+66}^{\text{eq}}$, stays roughly equal to 2 (Table I gives the typical value of 1.93 at 300 K). To illustrate this point, the computed traces of the Smith matrix (see Figs. 4 and 5 and the definition of the Smith matrix given in Appendix C) show many more peaks for ozone enriched in ^{18}O ($^{50}\text{O}_3^*$) than for ozone $^{48}\text{O}_3^*$. This implies a much higher density of metastable states for $^{50}\text{O}_3^*$ than for $^{48}\text{O}_3^*$. This increased density has a direct repercussion on K_{8+66}^{eq} , as explained in Appendix B, and thus on the concentration of $^{18}\text{O}^{16}\text{O}^{16}\text{O}^*$. The invoked statistical situation mentioned above would be without the asymmetry forced by the terminal ^{18}O atom in place of ^{16}O , dramatically increasing the density of states. In the statistical rules, what is expected is indeed purely a mass effect and we then speak of mass-dependent effect, while in what is calculated there is, added to this mass effect, a symmetry effect which manifests itself in the densities of states with many more metastable states of O_3^* for $^{50}\text{O}_3^*$ than

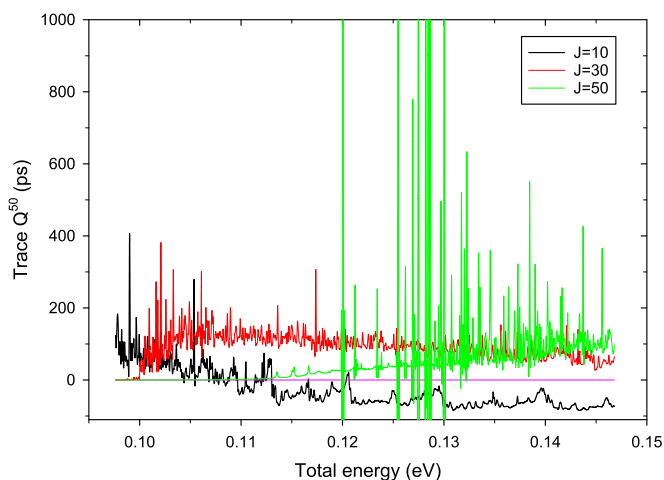


FIG. 5. Global lifetimes of $^{50}\text{O}_3^*$ complex, $\text{Tr } \mathbf{Q}_{50}^J(E)$, as a function of total energy E , for $J = 10, 30$, and 50 . The ordinate scale is cut at 1000 ps, but $\text{Tr } \mathbf{Q}_{50}^J(E)$ can be as high as 8000 ps for $J = 50$.

for $^{48}\text{O}_3^*$. The equilibrium constant for the other side process, $6 + 68$, keeps a value between $7 \times 10^{-23} \text{ cm}^3 \text{ molecule}^{-1}$ and around $5 \times 10^{-23} \text{ cm}^3 \text{ molecule}^{-1}$ for the whole range of temperatures, too close to the value of K_{6+66}^{eq} to influence the overall tendency. When we look at the formulas of $K_{6+66}^{\text{eq}}(T)$, $K_{8+66}^{\text{eq}}(T)$, $K_{6+68}^{\text{eq}}(T)$ given in Appendix B, the electronic partition function of the O_3^* complex, $z_{\text{O}_3^*}^{\text{el}}$, in the numerator is the same for all isotopes, whereas the rovibrational partition function for O_3^* , $z_{\text{O}_3^*}^{\text{rovib}}$, in the numerator and the expression of the reagents partition function, z^{reac} , change depending on the isotopomer considered. In z^{reac} , in the denominator, for the reagents, the electronic partition function, $z_{\text{O}-\text{O}_2}^{\text{el}}$, and the nuclear spin partition function, z^{ns} , are the same for all isotopes considered here. A value of roughly 2 is found for the ratio of diatomic rovibrational partition functions $z_{68}^{\text{rovib}}/z_{66}^{\text{rovib}}$. In Fig. 2 the main difference between $6 + 66$ and $8 + 66$ comes from the integral in the numerator of the formulas of $K_{6+66}^{\text{eq}}(T)$, $K_{8+66}^{\text{eq}}(T)$, $K_{6+68}^{\text{eq}}(T)$, the traces of the Smith matrix for $^{48}\text{O}_3^*$ and $^{50}\text{O}_3^*$ being very different (see Figs. 4 and 5).

Explicit values for these various quasiequilibrium constants are presented in Table I for the typical temperature $T = 300 \text{ K}$, along with their ratios with respect to the reference process $6 + 66$. For the $6 + 66$ equilibrium, we find a value of $6.74 \times 10^{-23} \text{ cm}^3 \text{ molecule}^{-1}$, slightly higher than the latest experimental estimation ($5 \times 10^{-23} \text{ cm}^3 \text{ molecule}^{-1}$, corrected from a much higher, older value of $8.33 \times 10^{-22} \text{ cm}^3 \text{ molecule}^{-1}$) by Kaufman and Kelso [23] and Klein and Herron [24,25], in a pioneering work dating back to the 1960s. Our computed value is, on the other hand, ten orders of magnitude lower than the surprisingly large one of $9.6 \times 10^{-13} \text{ cm}^3 \text{ molecule}^{-1}$ at $T = 400 \text{ K}$ obtained from kinetic models in 2005 by Luther *et al.* [17]. For $6 + 68$, our room temperature K^{eq} value of $4.84 \times 10^{-23} \text{ cm}^3 \text{ molecule}^{-1}$ is roughly one order of magnitude larger than that ($2.63 \times 10^{-24} \text{ cm}^3 \text{ molecule}^{-1}$ at $T = 300 \text{ K}$) calculated by Ivanov and Babikov [27], based on a mixed quantum-classical method. The discrepancy may result from their computation of the partition functions, susceptible of missing resonance states. We stress that we compute the density of rovibrational states of the complex O_3^* with a quantum method, including in principle all resonance states, regardless of their symmetry. Also shown in Table I are expected values of k^{stab} based on experimental data concerning k^{rec} , as mentioned in the Introduction with the hypothesis of the $k^{\text{rec}} = K^{\text{eq}} k^{\text{stab}}$ relation, together with their respective ratios to the reference formation process involving only ^{16}O atoms. These values have in no way been computed from any O_3^* stabilization model. As they stand, they must be considered as purely indicative. However, they are based on reliable experimental data [8–10] on k^{rec} and our accurately computed values of K^{eq} . They are given for specific formation rates of the various ozone isotopologues including one ^{18}O atom.

To begin with, for the reference $666^* + M$ process, our k^{stab} value ($8.98 \times 10^{-12} \text{ cm}^3 \text{ molecule}^{-1} \text{ s}^{-1}$) is very close to the experimental estimation ($10^{-11} \text{ cm}^3 \text{ molecule}^{-1} \text{ s}^{-1}$) first obtained by Kaufman and Kelso [23]. Compared to previous theoretical works using approximate approaches, our computed value is lower than that of Charlo and Clary ($4.92 \times 10^{-11} \text{ cm}^3 \text{ molecule}^{-1} \text{ s}^{-1}$) [29], Ivanov and Schinke

TABLE I. Room temperature (300 K) values for theoretical quasiequilibrium constants K^{eq} , experimental recombination process kinetic constant k^{rec} , and derived stabilization process constants k^{stab} , for the various indicated channels, with their ratios to the reference process 6 + 66.

$T = 300 \text{ K}$	6 + 66 (666)	8 + 66 (866)	6 + 68 (866)	6 + 68 (686)
K^{eq} ($\text{cm}^3 \cdot \text{molecule}^{-1}$) (Theory)	6.74×10^{-23}	1.30×10^{-22}		4.84×10^{-23}
k^{rec} ($\text{cm}^6 \cdot \text{molecule}^{-2} \cdot \text{s}^{-1}$) (Exp.)	6.05×10^{-34}	5.57×10^{-34}	4.39×10^{-34}	3.27×10^{-34}
k^{stab} ($\text{cm}^3 \cdot \text{molecule}^{-1} \cdot \text{s}^{-1}$)	8.98×10^{-12}	4.28×10^{-12}	9.07×10^{-12}	6.76×10^{-12}
$K^{\text{eq}}/K_{6+66}^{\text{eq}}$ ratio	1	1.930		0.718
$k^{\text{rec}}/k_{6+66}^{\text{rec}}$ ratio	1	0.921	0.725	0.540
$k^{\text{stab}}/k_{6+66}^{\text{stab}}$ ratio	1	0.477	1.010	0.752

($3.69 \times 10^{-11} \text{ cm}^3 \text{ molecule}^{-1} \text{ s}^{-1}$) [16] and Teplukhin and Babikov ($1.48 \times 10^{-10} \text{ cm}^3 \text{ molecule}^{-1} \text{ s}^{-1}$) [28], and larger than that of Schinke and Fleurat-Lessard ($10^{-13} - 5 \times 10^{-12} \text{ cm}^3 \text{ molecule}^{-1} \text{ s}^{-1}$) [33]. For the $686^* + M$ process, our value of k^{stab} for the specific symmetric isotopologue formation rate ($6.76 \times 10^{-12} \text{ cm}^3 \text{ molecule}^{-1} \text{ s}^{-1}$) has to be compared to that ($7.5 \times 10^{-14} \text{ cm}^3 \text{ molecule}^{-1} \text{ s}^{-1}$) of Ivanov and Babikov [27], and found two orders of magnitude greater. For 8 + 66, our value ($4.28 \times 10^{-12} \text{ cm}^3 \text{ molecule}^{-1} \text{ s}^{-1}$) compares to that ($5.90 \times 10^{-11} \text{ cm}^3 \text{ molecule}^{-1} \text{ s}^{-1}$) of Charlo and Clary [29], the latter remaining more than one order of magnitude higher. All these previously published results for the most part of theoretical nature point the difficulty in obtaining a reliable value of k^{stab} . Deactivation from a resonant state, or even from a highly excited rovibrational state, to lead to a stable species, is most likely a multistep process, not amenable to any simplifying treatment, such as the strong collision approximation [17]. Only approximate methods have been used for the k^{stab} estimation so far. The accurate treatment of step (1a) we bring here thus permits, indirectly, the setting of a benchmark value for k^{stab} , definitely assessing the validity of different future models and methods for its estimation.

Figure 3 allows one to gain further information on the equilibrium process with respect to the total angular momentum J components of K^{eq} . The K^{eq} components for the 6 + 66 equilibrium behave very differently from one another. It immediately appears that all J values are needed for a reliable computation of K^{eq} , whatever the temperature range. The sharply oscillating behavior with consecutive middle-range J values was not predictable, even though the overall shape appears as a common monomodal distribution with an extended right wing. On the other hand, the small and near zero values of K^{eq} components, respectively, at very low J ($J < 3$) and high J ($J > 70$), were expected. The diminishing contribution with increasing J obviously reveals the convergence for the partial J -wave expansion for lifetime matrix \mathbf{Q} . Any tentative interpolation from an incomplete set of J values is therefore doomed to fail. Components are consistently ordered [$K^{\text{eq}}(T = 200) > K^{\text{eq}}(T = 250) > K^{\text{eq}}(T = 300)$] for all J values below roughly 40, then tend to merge for all higher J values. The highest peaks are obtained at the lowest temperature (200 K in Fig. 3). This behavior is confirmed for the 8 + 66 and 6 + 68 equilibria, as can be seen in Figs. 9 and 10. These results clearly indicate that an

isotope effect, not solely due to mass change but originating from the alteration of the density of resonance states, when moving from 666^* to 866^* , especially for middle range to high J values, is already present in the fast quasiequilibrium (1a). Its combination to another, hypothetical one, in the stabilization step (1b), however, much more difficult to describe with the same level of accuracy, would lead to a complete explanation of the MIF observed for ^{18}O mono-substituted ozone in stratospheric conditions or in laboratory experiments.

IV. CONCLUSION

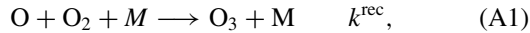
This study reports reliable quantitative information on the first step (1a) of ozone formation reaction (1) involved in the MIF. Accurate values of the quasiequilibrium constant K^{eq} for (1a) were computed using a full QM method and can therefore serve as reference values. Detailed quantum characterization of this process reveals important isotope effects as well as the role played by a large number of total angular momenta, proving the need for a complete description of this process. These findings, as they appear to be in good agreement with the scarce experimental data available from the 1960s, might stimulate new experiments, even if they do not seem easy to carry out. Our results can also be used as reference for improving the modeling and simulation methods of the second step (1b) that is the deactivation of excited ozone O_3^* . Accurate determination of the stabilization constant k^{stab} for (1b) has not been achieved so far and this is the next challenge to be addressed. In view of the ozone MIF long-standing issue, the combination of the present results with a proper quantum description of this second step, with and without isotopic substitution, would lead to a full understanding of this open question, and perhaps finally find an answer to the MIF mystery.

ACKNOWLEDGMENTS

All computations were performed using HPC resources from DNUM CCUB (Centre de Calcul de l'Université de Bourgogne). We thank E. Privat for his contribution to the extension of the quantum scattering code dedicated to lifetimes computation. We thank R. Kochanov and V. Tyuterev for sending us the O_3 potential energy surface.

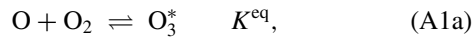
APPENDIX A: QUASIEQUILIBRIUM IN ENERGY TRANSFER (LINDEMANN) MECHANISM

We consider the ozone forming recombination reaction



where k^{rec} is the total (third order) recombination rate constant.

The Lindemann (energy transfer) approximating mechanism consists in two separate steps:

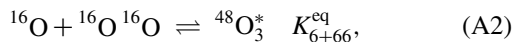


The first step, Eq. (A1a), can be considered as a quasiequilibrium between reactants $\text{O} + \text{O}_2$ and metastable states O_3^* characterized by equilibrium constant K^{eq} . Regarding the second step, Eq. (A1b), k^{stab} is the average rate coefficient for the deactivation, or stabilization, of O_3^* .

We now separate processes involving only ^{16}O isotopes from those in which a heavy oxygen ^{18}O isotope is present.

Note: In the following, we will frequently use an abbreviated notation: we will write “6” for ^{16}O , “8” for ^{18}O , “66” for $^{16}\text{O}^{16}\text{O}$ and so on.

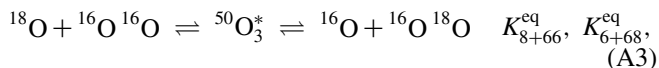
We thus consider first



with equilibrium constant

$$K_{6+66}^{\text{eq}} = \frac{[^{48}\text{O}_3^*]}{[^{16}\text{O}][^{16}\text{O}^{16}\text{O}]},$$

and then the two-sided quasiequilibrium



with two distinct equilibrium constants respectively given by

$$K_{8+66}^{\text{eq}} = \frac{[^{50}\text{O}_3^*]_{\text{as}}}{[^{18}\text{O}][^{16}\text{O}^{16}\text{O}]}$$

and

$$K_{6+68}^{\text{eq}} = \frac{[^{50}\text{O}_3^*]_{\text{as+s}}}{[^{16}\text{O}][^{16}\text{O}^{18}\text{O}]}.$$

In the above equations, $[^{50}\text{O}_3^*]_{\text{as}}$ refers to the concentration of metastable complexes of the asymmetric 866* (“as” or “ C_s symmetry”) type, while $[^{50}\text{O}_3^*]_{\text{as+s}}$ includes both asymmetric and symmetric 686* (“s” or “ C_{2v} symmetry”) types, even if this point group classification picture is not especially adapted for resonance states (see Fig. 1).

APPENDIX B: PARTITION FUNCTIONS AND RESONANCE STATE DENSITIES

1. Case of $^{48}\text{O}_3$

These quasiequilibrium constants can be expressed with the help of reagents $\text{O} + \text{O}_2$ and intermediate complex O_3^*

partition functions $z(T)$. We have, for the 6 + 66 case,

$$\begin{aligned} K_{6+66}^{\text{eq}}(T) &= \frac{z_{666^*}^{\text{eq}}}{z_{6+66}^{\text{eq}}} = \frac{z_{\text{O}_3}^{\text{el}} z_{666^*}^{\text{rovib-ns}} z_{48\text{O}_3}^{\text{ns}}}{z_{\text{O}-\text{O}_2}^{\text{el}} z_{66}^{\text{rovib}} z_{6+66}^{\text{tr}} z_{6+66}^{\text{ns}}} \\ &= \frac{z_{\text{O}_3}^{\text{el}} z_{666^*}^{\text{rovib}}}{z_{\text{O}-\text{O}_2}^{\text{el}} z_{66}^{\text{rovib}} z_{6+66}^{\text{tr}}} \end{aligned}$$

taking the energy origin at the bottom of the diatomic O_2 potential well.

This quantity was plotted in Fig. 2.

Here we have for the reactants 6 + 66 electronic partition function [47]:

$$z_{\text{O}-\text{O}_2}^{\text{el}}(T) = 3[5 + 3 e^{-227.6/T} + e^{325.9/T}]$$

$$z_{66}^{\text{rovib}}(T) = \sum_{j=1,3,\dots} (2j+1) e^{-\beta \epsilon_{v=0,j}},$$

with $\beta \equiv 1/(k_B T)$, k_B being the Boltzmann constant, and where $\epsilon_{v=0,j}$ are accurately computed rovibrational energies of 66, restricted, for absolute temperature $T < 400$ K, to fundamental rovibrational level $v = 0$.

The reagents relative translation partition function is simply

$$z_{6+66}^{\text{tr}}(T) = \Lambda_{6+66}^{-3}(T),$$

with $\Lambda_{6+66}(T) = \frac{h}{\sqrt{2\pi \mu_{6+66} k_B T}}$ is the thermal wavelength for 6 + 66 (with μ_{6+66} the reduced mass and $h = 2\pi \hbar$ the Planck constant).

The nuclear spin for 6 is zero, so we have only one nuclear spin state and the nuclear spin partition functions for complex and reagents are $z_{48\text{O}_3}^{\text{ns}} = z_{6+66}^{\text{ns}} = 1$. Also, the dynamics happens on the lowest of the 27 spin-orbit coupled electronic states merging asymptotically, so we use an approximate expression for the O_3^* complex electronic partition function valid in the neighborhood of equilibrium geometry [30] based on fine-structure *ab initio* calculations [48], including nine terms with Σ and Π symmetries and spin multiplicity from 1 to 5:

$$\begin{aligned} z_{\text{O}_3^*}^{\text{el}}(T) &= 1 + e^{-213/T} + 3 e^{-242/T} + 3 e^{-410/T} + 5 e^{-699/T} \\ &\quad + 5 e^{-823/T} + 5 e^{-1429/T} + e^{-1500/T} + 3 e^{-1522/T}. \end{aligned}$$

The metastable complex rovibrational partition function is estimated with the help of the trace of the Smith \mathbf{Q} matrix [44] (see Appendix C):

$$\begin{aligned} z_{666^*}^{\text{rovib}}(T) &= \mathcal{L} \left[\sum_J (2J+1) \rho_{666^*}^J(E) \right] \\ &= (2\pi \hbar)^{-1} \sum_J (2J+1) \\ &\quad \times \int_0^\infty \text{Tr} \mathbf{Q}_{666^*}^J(E) \exp(-\beta E) dE, \end{aligned}$$

where $E = E_{c(vj)} + \epsilon_{vj}$ is the total energy [ϵ_{vj} being internal diatomic rovibration energy and $E_{c(vj)}$ being the collision energy relative to (vj) level], where J is the total angular momentum of the complex, and $\mathcal{L}[\bullet]$ denotes the Laplace transform. $\text{Tr} \mathbf{Q}_{666^*}^J(E)$ denotes the trace of the \mathbf{Q} matrix

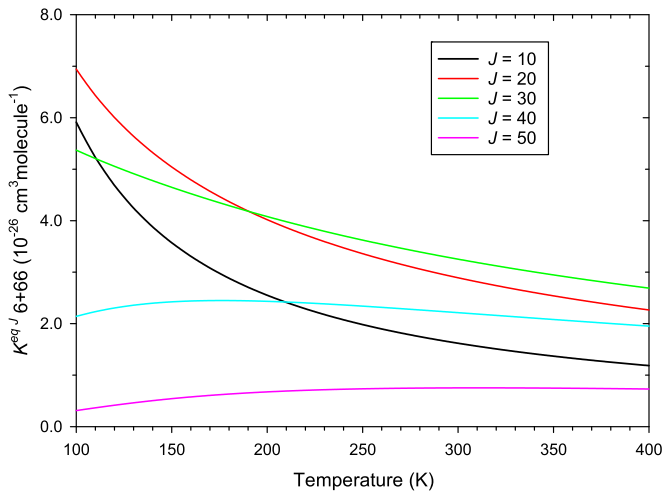


FIG. 6. Total angular momentum J components for the quasiequilibrium constant $K_{6+66}^{eq,J}$ as a function of temperature T , for the $6 + 66$ reference process, for various total angular momenta $J = 10, 20, 30, 40$, and 50 , for a range of temperatures between 100 and 400 K.

computed at energy E . We, of course, have $\mathbf{Q}_{666}^J(E) = \mathbf{0}$ for $E_{c(v_j)} < 0$.

This formula is transparent for the case of sufficiently narrow resonances with lorentzian shapes. Indeed, the density of resonance states can be expressed using the trace of the \mathbf{Q} -matrix [49]

$$\rho_{666}^J(E) = (2\pi\hbar)^{-1} \text{Tr} \mathbf{Q}_{666}^J(E).$$

It can otherwise be derived on quite rigorous grounds with the help of the Fredholm determinant [50–53]. We arrive in this way at the same result obtained by Smith [54,55] and Bowman [56] in slightly different fashions.

We can thus assemble the whole, following the notations in Ref. [57], as

$$K_{6+66}^{eq}(T) = \sum_J K_{6+66}^{eq,J}(T),$$

with

$$K_{6+66}^{eq,J}(T) = \frac{z_{\text{O}_3}^{\text{el}}}{z_{6+66}^{\text{reac}}} (2\pi\hbar)^{-1} (2J+1) \times \int_0^\infty \text{Tr} \mathbf{Q}_{666}^J(E) \exp(-\beta E) dE.$$

Examples of quantities $K_{6+66}^{eq,J}(T)$ are plotted in Figs. 6 and 3.

2. Case of $^{50}\text{O}_3$

As the $^{50}\text{O}_3^*$ complex is related to two different sets of reagents (see Fig. 1), we need to separate between partition functions (sum over states) for the symmetric and asymmetric complexes.

Similarly to the $^{48}\text{O}_3$ case, we have

$$K_{8+66}^{\text{eq}}(T) = \frac{z_{866}^*}{z_{8+66}^{\text{reac}}} = \frac{z_{\text{O}_3}^{\text{el}} z_{866}^{\text{rovib,ns}}}{z_{\text{O-O}_2}^{\text{el}} z_{66}^{\text{rovib,tr}} z_{8+66}^{\text{tr}} z_{8+66}^{\text{ns}}} \\ = \frac{z_{\text{O}_3}^{\text{el}} z_{866}^{\text{rovib}}}{z_{\text{O-O}_2}^{\text{el}} z_{66}^{\text{rovib,tr}} z_{8+66}^{\text{tr}}}$$

and

$$K_{6+68}^{\text{eq}}(T) = \frac{\frac{1}{2}(z_{686}^* + z_{866}^*)}{z_{6+68}^{\text{reac}}} \\ = \frac{z_{\text{O}_3}^{\text{el}} \left(\frac{1}{2} z_{686}^{\text{rovib}} + \frac{1}{2} z_{866}^{\text{rovib}} \right) z_{50\text{O}_3}^{\text{ns}}}{z_{\text{O-O}_2}^{\text{el}} z_{68}^{\text{rovib,tr}} z_{6+68}^{\text{tr}} z_{6+68}^{\text{ns}}} \\ = \frac{z_{\text{O}_3}^{\text{el}} \left(\frac{1}{2} z_{686}^{\text{rovib}} + \frac{1}{2} z_{866}^{\text{rovib}} \right)}{z_{\text{O-O}_2}^{\text{el}} z_{68}^{\text{rovib,tr}} z_{6+68}^{\text{tr}}},$$

with again $z_{50\text{O}_3}^{\text{ns}} = z_{8+66}^{\text{ns}} = z_{6+68}^{\text{ns}} = 1$. These quantities were also plotted in Fig. 2. In these expressions we neglect the so-called “roaming” phenomenon [58] and take account of the fact that the second equilibrium involves both symmetric and asymmetric complexes with equal probabilities, while the first involves asymmetric species only.

Again, we have the same electronic partition function $z_{\text{O-O}_2}^{\text{el}}(T)$ as before, and the rovibrational part is

$$z_{68}^{\text{rovib}}(T) = \sum_{j=0,1,2,\dots} (2j+1) e^{-\beta \varepsilon_{v=0,j}},$$

where $\varepsilon_{v=0,j}$ are this time accurately computed rovibrational energies of 68, restricted for $T < 400$ K to $v = 0$.

The relative translation partition functions

$$z_{8+66}^{\text{tr}}(T) = \Lambda_{8+66}^{-3}(T) \quad \text{and} \quad z_{6+68}^{\text{tr}}(T) = \Lambda_{6+68}^{-3}(T)$$

have exactly similar expressions as z_{6+66}^{tr} , just changing the reduced masses.

The partition functions for the complexes, distinguishing between “asymmetric” and “symmetric,” are formally written

$$z_{866}^{\text{rovib}}(T) = \mathcal{L} \left[\sum_J (2J+1) \rho_{866}^J(E) \right] \\ = (2\pi\hbar)^{-1} \sum_J (2J+1) \\ \times \int_0^\infty \text{Tr}' \mathbf{Q}_{866}^J(E) \exp(-\beta E) dE,$$

and

$$z_{686}^{\text{rovib}}(T) = \mathcal{L} \left[\sum_J (2J+1) \rho_{686}^J(E) \right] \\ = (2\pi\hbar)^{-1} \sum_J (2J+1) \\ \times \int_0^\infty \text{Tr}' \mathbf{Q}_{686}^J(E) \exp(-\beta E) dE,$$

where the notation Tr' stands for a partial trace restricted to the “correct” symmetry. Of course we have

$$\text{Tr}' \mathbf{Q}_{866}^J(E) + \text{Tr}' \mathbf{Q}_{686}^J(E) = \text{Tr} \mathbf{Q}_{50}^J(E).$$

At this point we need to make a further assumption, which is that the number of asymmetric states is roughly the double of that of symmetric states [59]

$$[{}^{50}\text{O}_3^*]_{\text{as}} \approx 2[{}^{50}\text{O}_3^*]_{\text{s}},$$

that is

$$[{}^{18}\text{O}{}^{16}\text{O}{}^{16}\text{O}^*] \approx 2[{}^{16}\text{O}{}^{18}\text{O}{}^{16}\text{O}^*]$$

Remembering that $[{}^{50}\text{O}_3^*]_{\text{as}} + [{}^{50}\text{O}_3^*]_{\text{s}} = [{}^{18}\text{O}{}^{16}\text{O}{}^{16}\text{O}^*] + [{}^{16}\text{O}{}^{18}\text{O}{}^{16}\text{O}^*] = [{}^{50}\text{O}_3^*]$, we obtain

$$\begin{aligned} [{}^{18}\text{O}{}^{16}\text{O}{}^{16}\text{O}^*] &= [{}^{50}\text{O}_3^*]_{\text{as}} = \frac{2}{3}[{}^{50}\text{O}_3^*] \quad \text{and} \quad [{}^{16}\text{O}{}^{18}\text{O}{}^{16}\text{O}^*] \\ &= [{}^{50}\text{O}_3^*]_{\text{s}} = \frac{1}{3}[{}^{50}\text{O}_3^*]. \end{aligned}$$

This reflects directly on complexes partition functions

$$z_{866^*}^{\text{rovib}} = \frac{2}{3}z_{50^*}^{\text{rovib}}$$

and

$$z_{686^*}^{\text{rovib}} = \frac{1}{3}z_{50^*}^{\text{rovib}},$$

where $z_{50^*}^{\text{rovib}}$ is directly obtained from the total trace of the lifetime matrix for the ${}^{50}\text{O}_3^*$ system

$$\begin{aligned} z_{50^*}^{\text{rovib}}(T) &= \mathcal{L} \left[\sum_J (2J+1) \rho_{50^*}^J(E) \right] \\ &= (2\pi\hbar)^{-1} \sum_J (2J+1) \\ &\quad \times \int_0^\infty \text{Tr} \mathbf{Q}_{50^*}^J(E) \exp(-\beta E) dE. \end{aligned}$$

We explicitly computed the quantity $\text{Tr} \mathbf{Q}_{50^*}^J(E)$ with the dedicated subroutine [45,46] of our time-independent QM [35,36].

We can thus express, formally

$$K_{8+66}^{\text{eq}}(T) = \sum_J K_{8+66}^{\text{eq}'}(T),$$

with

$$\begin{aligned} K_{8+66}^{\text{eq}'}(T) &= \frac{z_{\text{O}_3}^{\text{el}}}{z_{8+66}^{\text{react}}} (2\pi\hbar)^{-1} (2J+1) \\ &\quad \times \int_0^\infty \text{Tr}' \mathbf{Q}_{866^*}^J(E) \exp(-\beta E) dE. \end{aligned}$$

Examples of such quantities $K_{8+66}^{\text{eq}'}(T)$ are plotted in Figs. 7 and 9.

Similarly,

$$K_{6+68}^{\text{eq}}(T) = \sum_J K_{6+68}^{\text{eq}'}(T),$$

with

$$\begin{aligned} K_{6+68}^{\text{eq}'}(T) &= \frac{z_{\text{O}_3}^{\text{el}}}{z_{6+68}^{\text{react}}} (2\pi\hbar)^{-1} (2J+1) \\ &\quad \times \int_0^\infty \text{Tr}' \mathbf{Q}_{686^*}^J(E) \exp(-\beta E) dE. \end{aligned}$$

As an example, quantities $K_{6+68}^{\text{eq}'}(T)$, as a function of temperature and total angular momentum J , are represented in Figs. 8 and 10.

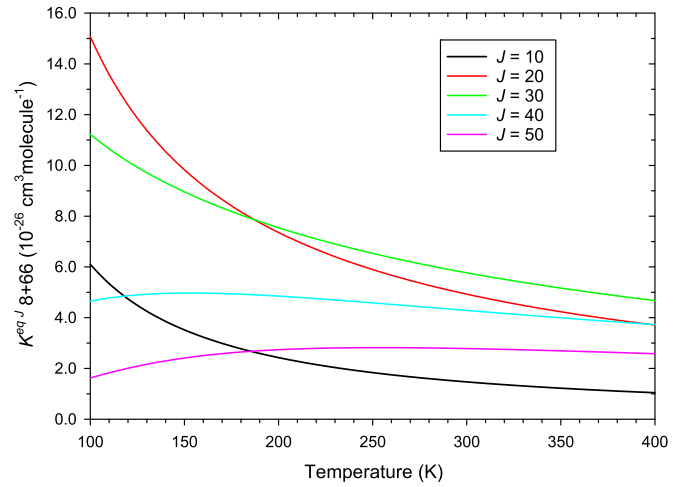


FIG. 7. Total angular momentum J components for the quasiequilibrium constant $K_{8+66}^{\text{eq}'}(T)$ as a function of temperature T , for the $8 + 66$ process, for various total angular momenta $J = 10, 20, 30, 40$, and 50 , for a range of temperatures between 100 and 400 K.

APPENDIX C: DEFINITION OF Q MATRIX

We start from the following definition by Smith [44]

$$\mathbf{Q}(E) = -i\hbar\mathbf{S}^\dagger \frac{d\mathbf{S}}{dE} = i\hbar\mathbf{S} \frac{d\mathbf{S}^\dagger}{dE} = \mathbf{Q}^\dagger(E),$$

where \mathbf{S} is the unitary scattering matrix (the same we use for the computation of cross sections), and \mathbf{Q} is hermitian, therefore its eigenvalues and trace are real.

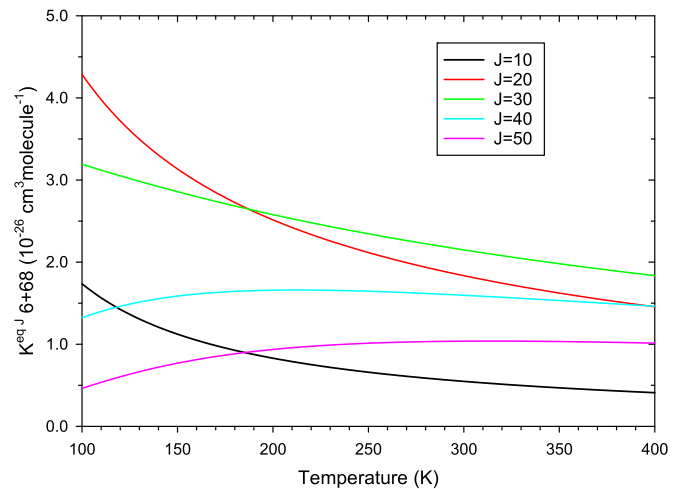


FIG. 8. Total angular momentum J components for the quasiequilibrium constant $K_{6+68}^{\text{eq}'}(T)$ as a function of temperature T , for the $6 + 68$ process, for various total angular momenta $J = 10, 20, 30, 40$, and 50 , for a range of temperatures between 100 and 400 K.

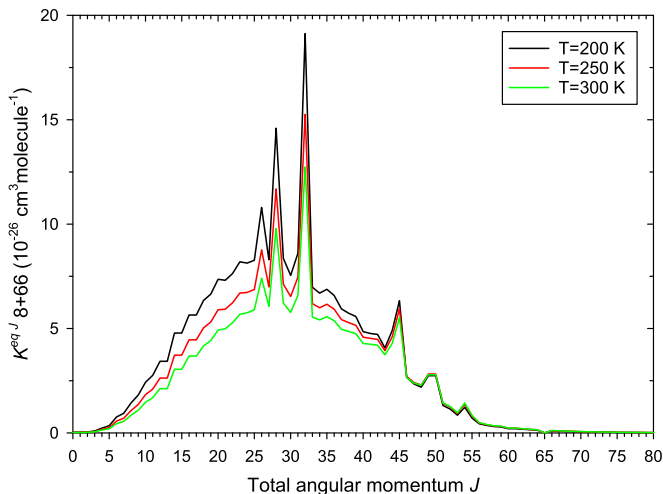


FIG. 9. Equilibrium constant J components, K_{8+66}^{eq} , as a function of total angular momentum J , for three different temperatures: $T = 200$ K, $T = 250$ K, and $T = 300$ K.

As the \mathbf{S} matrix is bloc-diagonal in total angular momentum J , we can work in J -labelled blocs:

$$\mathbf{Q}^J(E) = -i\hbar \mathbf{S}^{J\dagger} \frac{d\mathbf{S}^J}{dE}.$$

Details of the algorithm for the computation of $\mathbf{Q}(E)$ alongside with $\mathbf{S}(E)$, by using a modification [60–63] of the log-derivative propagation algorithm [64,65], in the same spirit as with \mathbf{R} -matrix [66,67], are given in Refs. [45,46].

In a formal fashion, a diagonal element $Q_{nn}^J(E)$ is the average lifetime of a collision (reactive or not) starting with initial channel n . In space-fixed representation for collision dynamics we would have $n = (vj\Omega)$ with v being the initial diatomic vibration quantum number (for the temperatures considered here we always have $v = 0$), j the initial diatomic rotation quantum number, l the initial relative orbital angular momentum quantum number. We thus start with \mathbf{Q} -matrix diagonal elements: $Q_{vj\Omega;vj\Omega}^J(E)$.

We actually work in a body-fixed representation, so the l quantum number is replaced by Ω , which is the triatomic O_3 total angular momentum projection on least inertia axis,

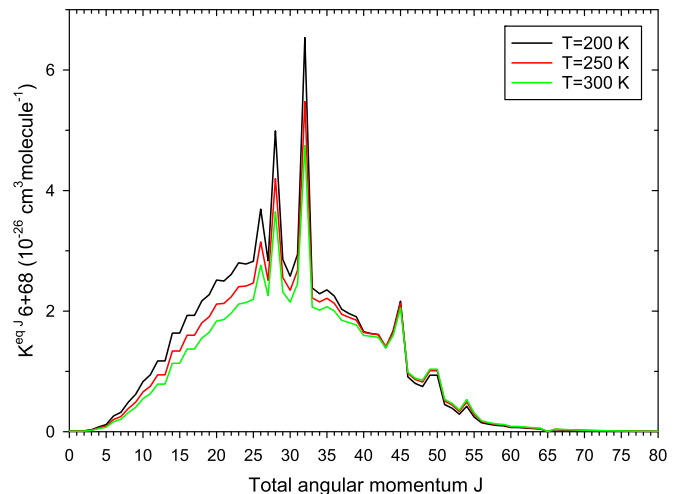


FIG. 10. Equilibrium constant J components, K_{6+68}^{eq} , as a function of total angular momentum J , for three different temperatures: $T = 200$ K, $T = 250$ K, and $T = 300$ K.

such that $n = (vj\Omega)$. A diagonal \mathbf{Q} matrix element really is denoted as: $Q_{vj\Omega;vj\Omega}^J(E)$. The trace of the Smith matrix is simply computed as

$$\text{Tr } \mathbf{Q}^J(E) = \sum_{vj\Omega} Q_{vj\Omega;vj\Omega}^J(E).$$

For cases of sharply peaked values, this quantity very closely approximates eigenlifetimes $q_m^J(E)$ that would result from a diagonalization of the entire \mathbf{Q} -matrix, then giving genuine lifetimes of metastable complex O_3^* forming at energy E .

Note: In view of the above remark, and given that the density of states cannot be negative, a filtering of allowed lifetimes for the complex O_3^* has been made according to Heisenberg criteria [44]:

$$q_m^J(E) \approx \text{Tr } \mathbf{Q}^J(E) > \frac{\hbar}{2E}.$$

As an example, the quantities $\text{Tr } \mathbf{Q}^J(E)$, with no criteria, as a function of total energy, for various total angular momenta, are represented, for $^{48}\text{O}_3^*$ and $^{50}\text{O}_3^*$, in Figs. 4 and 5.

- [1] J. M. Carlstad and K. A. Boering, Isotope effects and the atmosphere, *Annu. Rev. Phys. Chem.* **74**, 439 (2023).
- [2] K. Mauersberger, Measurement of heavy ozone in the atmosphere, *Geophys. Res. Lett.* **8**, 935 (1981).
- [3] M. H. Thiemens and J. E. Heidenreich, III, The mass-independent fractionation of oxygen: A novel isotope effect and its possible cosmochemical implications, *Science* **219**, 1073 (1983).
- [4] M. H. Thiemens, S. Chakraborty, and G. Dominguez, The physical chemistry of mass-independent isotope effects and their observation in nature, *Annu. Rev. Phys. Chem.* **63**, 155 (2012).
- [5] K. Mauersberger, B. Erbacher, D. Krankowsky, J. Günther, and R. Nickel, Ozone isotope enrichment: Isotopomer-specific rate coefficients, *Science* **283**, 370 (1999).

- [6] J. E. Heidenreich, III and M. H. Thiemens, A non mass isotope effect in the production of ozone from molecular oxygen: The role of molecular symmetry in isotope chemistry, *J. Chem. Phys.* **84**, 2129 (1986).
- [7] S. M. Anderson, D. Hulsebusch, and K. Mauersberger, Surprising rate coefficients for four isotopic variants of $\text{O} + \text{O}_2 + \text{M}$, *J. Chem. Phys.* **107**, 5385 (1997).
- [8] C. Janssen, J. Guenther, D. Krankowsky, and K. Mauersberger, Relative formation rates of $^{50}\text{O}_3$ and $^{52}\text{O}_3$ in ^{16}O - ^{18}O mixtures, *J. Chem. Phys.* **111**, 7179 (1999).
- [9] C. Janssen, J. Guenther, K. Mauersberger, and D. Krankowsky, Kinetic origin of the ozone isotope effect: A critical analysis of enrichments and rate coefficients, *Phys. Chem. Chem. Phys.* **3**, 4718 (2001).

- [10] C. Janssen, J. Guenther, D. Krankowsky, and K. Mauersberger, Temperature dependence of ozone rate coefficients and isotopologue fractionation in ^{16}O – ^{18}O oxygen mixtures, *Chem. Phys. Lett.* **367**, 34 (2003).
- [11] B. C. Hathorn and R. A. Marcus, An intramolecular theory of the mass-independent isotope effect for ozone. I, *J. Chem. Phys.* **111**, 4087 (1999).
- [12] B. Hathorn and R. Marcus, An intramolecular theory of the mass-independent isotope effect for ozone. II. numerical implementation at low pressures using a loose transition state, *J. Chem. Phys.* **113**, 9497 (2000).
- [13] Y. Q. Gao and R. A. Marcus, Strange and unconventional isotope effects in ozone formation, *Science* **293**, 259 (2001).
- [14] Y. Q. Gao and R. A. Marcus, On the theory of the strange and unconventional isotopic effects in ozone formation, *J. Chem. Phys.* **116**, 137 (2002).
- [15] M. Mirahmadi, J. Pérez-Ríos, O. Egorov, V. Tyuterev, and V. Kokoouline, Ozone formation in ternary collisions: Theory and experiment reconciled, *Phys. Rev. Lett.* **128**, 108501 (2022).
- [16] M. V. Ivanov and R. Schinke, Recombination of ozone via the chaperon mechanism, *J. Chem. Phys.* **124**, 104303 (2006).
- [17] K. Luther, K. Oum, and J. Troe, The role of the radical-complex mechanism in the ozone recombination/dissociation reaction, *Phys. Chem. Chem. Phys.* **7**, 2764 (2005).
- [18] D. Babikov, B. K. Kendrick, R. B. Walker, R. Schinke, and R. T. Pack, Quantum origin of an anomalous isotope effect in ozone formation, *Chem. Phys. Lett.* **372**, 686 (2003).
- [19] R. Schinke, P. Fleurat-Lessard, and S. Y. Grebenshchikov, Isotope dependence of the lifetime of ozone complexes formed in $\text{O} + \text{O}_2$ collisions, *Phys. Chem. Chem. Phys.* **5**, 1966 (2003).
- [20] P. Reinhardt and F. Robert, Mass independent isotope fractionation in ozone, *Earth Planet. Sci. Lett.* **368**, 195 (2013).
- [21] P. Reinhardt and F. Robert, On the mass independent isotope fractionation in ozone, *Chem. Phys.* **513**, 287 (2018).
- [22] V. Kokoouline, D. Lapierre, A. Alijah, and V. Tyuterev, Localized and delocalized bound states of the main isotopologue $^{48}\text{O}_3$ and of ^{18}O -enriched $^{50}\text{O}_3$ isotopomers of the ozone molecule near the dissociation threshold, *Phys. Chem. Chem. Phys.* **22**, 15885 (2020).
- [23] F. Kaufman and J. R. Kelso, M effect in the gas-phase recombination of O with O_2 , *J. Chem. Phys.* **46**, 4541 (1967).
- [24] F. S. Klein and J. T. Herron, Mass-spectrometric study of the reactions of O atoms with NO and NO_2 , *J. Chem. Phys.* **41**, 1285 (1964).
- [25] F. S. Klein and J. T. Herron, Erratum: Mass spectrometric study of the reactions of O atoms with NO and NO_2 , *J. Chem. Phys.* **44**, 3645 (1966).
- [26] R. Schinke and P. Fleurat-Lessard, The effect of zero-point energy differences on the isotope dependence of the formation of ozone: A classical trajectory study, *J. Chem. Phys.* **122**, 094317 (2005).
- [27] M. V. Ivanov and D. Babikov, Collisional stabilization of van der Waals states of ozone, *J. Chem. Phys.* **134**, 174308 (2011).
- [28] A. Teplukhin and D. Babikov, A full-dimensional model of ozone forming reaction: The absolute value of the recombination rate coefficient, its pressure and temperature dependencies, *Phys. Chem. Chem. Phys.* **18**, 19194 (2016).
- [29] D. Charlo and D. C. Clary, Quantum-mechanical calculations on termolecular association reactions $\text{XY} + \text{Z} + \text{M} \rightarrow \text{XYZ} + \text{M}$: Application to ozone formation, *J. Chem. Phys.* **117**, 1660 (2002).
- [30] D. Charlo and D. C. Clary, Quantum-mechanical calculations on pressure and temperature dependence of three-body recombination reactions: Application to ozone formation rates, *J. Chem. Phys.* **120**, 2700 (2004).
- [31] T. Xie and J. M. Bowman, Quantum inelastic scattering study of isotope effects in ozone stabilization dynamics, *Chem. Phys. Lett.* **412**, 131 (2005).
- [32] S. Sur, S. A. Ndengué, E. Quintas-Sánchez, C. Bop, F. Lique, and R. Dawes, Rotationally inelastic scattering of O_3 -Ar: State-to-state rates with the multiconfigurational time dependent Hartree method, *Phys. Chem. Chem. Phys.* **22**, 1869 (2020).
- [33] R. Schinke, S. Y. Grebenshchikov, M. V. Ivanov, and P. Fleurat-Lessard, Dynamical studies of the ozone isotope effect: A status report, *Annu. Rev. Phys. Chem.* **57**, 625 (2006).
- [34] R. A. Marcus, Theory of mass-independent fractionation of isotopes, phase space accessibility, and a role of isotopic symmetry, *Proc. Natl. Acad. Sci. USA* **110**, 17703 (2013).
- [35] J. M. Launay and M. L. Dourneuf, Hyperspherical close-coupling calculation of integral cross sections for the reaction $\text{H} + \text{H}_2 \rightarrow \text{H}_2 + \text{H}$, *Chem. Phys. Lett.* **163**, 178 (1989).
- [36] P. Honvault and J.-M. Launay, Quantum dynamics of insertion reactions, in *Theory of Chemical Reaction Dynamics*, edited by A. Lagana and G. Lendvay (Springer, Dordrecht, The Netherlands, 2004), pp. 187–215.
- [37] V. G. Tyuterev, R. V. Kochanov, S. A. Tashkun, F. Holka, and P. G. Szalay, New analytical model for the ozone electronic ground state potential surface and accurate *ab initio* vibrational predictions at high energy range, *J. Chem. Phys.* **139**, 134307 (2013).
- [38] V. G. Tyuterev, R. Kochanov, A. Campargue, S. Kassi, D. Mondelain, A. Barbe, E. Starikova, M. R. De Backer, P. G. Szalay, and S. Tashkun, Does the “reef structure” at the ozone transition state towards the dissociation exist? new insight from calculations and ultrasensitive spectroscopy experiments, *Phys. Rev. Lett.* **113**, 143002 (2014).
- [39] D. Lapierre, A. Alijah, R. Kochanov, V. Kokoouline, and V. Tyuterev, Lifetimes and wave functions of ozone metastable vibrational states near the dissociation limit in a full-symmetry approach, *Phys. Rev. A* **94**, 042514 (2016).
- [40] G. Guillon, P. Honvault, R. Kochanov, and V. Tyuterev, First-principles computed rate constant for the $\text{O} + \text{O}_2$ isotopic exchange reaction now matches experiment, *J. Phys. Chem. Lett.* **9**, 1931 (2018).
- [41] M. T. Cvitaš, P. Soldán, J. M. Hutson, P. Honvault, and J.-M. Launay, Ultracold collisions involving heteronuclear alkali metal dimers, *Phys. Rev. Lett.* **94**, 200402 (2005).
- [42] P. Honvault, M. Jorfi, T. Gonzalez-Lezana, A. Faure, and L. Pagani, Ortho-para H_2 conversion by proton exchange at low temperature: An accurate quantum mechanical study, *Phys. Rev. Lett.* **107**, 023201 (2011).
- [43] J. Daranlot, M. Jorfi, C. Xie, A. Bergeat, M. Costes, P. Caubet, D. Xie, H. Guo, P. Honvault, and K. Hickson, Revealing atom-radical reactivity at low temperature through the $\text{N} + \text{OH}$ reaction, *Science* **334**, 1538 (2011).
- [44] F. T. Smith, Lifetime matrix in collision theory, *Phys. Rev.* **118**, 349 (1960).

- [45] E. Privat, G. Guillon, and P. Honvault, Extension of the Launay quantum reactive scattering code and direct computation of time delays, *J. Chem. Theory Comput.* **15**, 5194 (2019).
- [46] E. Privat, G. Guillon, and P. Honvault, Direct time delay computation applied to the $O + O_2$ exchange reaction at low energy: Lifetime spectrum of O_3^* species, *J. Chem. Phys.* **154**, 104303 (2021).
- [47] A. Gross and G. D. Billing, Isotope effects on the rate constants for the processes $O_2 + O \rightarrow O + O_2$ and $O_2 + O + Ar \rightarrow O_3 + Ar$ on a modified ground-state potential energy surface for ozone, *Chem. Phys.* **217**, 1 (1997).
- [48] P. Rosmus, P. Palmieri, and R. Schinke, The asymptotic region of the potential energy surfaces relevant for the $O + O_2 \rightarrow O_3$ reaction, *J. Chem. Phys.* **117**, 4871 (2002).
- [49] K. Takahashi, M. Y. Hayes, and R. T. Skodje, A study of resonance progressions in the $F + HCl \rightarrow Cl + HF$ reaction: A lifetime matrix analysis of pre-reactive and post-reactive collision complexes, *J. Chem. Phys.* **138**, 024309 (2013).
- [50] R. G. Newton, *Scattering Theory of Waves and Particles*, 2nd ed., Dover Books on Physics (Dover, Mineola, NY, 2002).
- [51] R. D. Levine, *Quantum Mechanics of Molecular Rate Processes*, Dover Books on Chemistry (Dover, Mineola, NY, 1999).
- [52] M. Baker, Determinantal approach to meson-nucleon scattering, *Ann. Phys. (NY)* **4**, 271 (1958).
- [53] B. S. DeWitt, Transition from discrete to continuous spectra, *Phys. Rev.* **103**, 1565 (1956).
- [54] F. T. Smith, Collision lifetimes and the thermodynamics of real gases, *J. Chem. Phys.* **38**, 1304 (1963).
- [55] F. T. Smith, Collision lifetimes in many-body processes, *Phys. Rev.* **130**, 394 (1963).
- [56] J. M. Bowman, Collision lifetime approach to recombination and a new derivation of RRKM theory, *J. Phys. Chem.* **90**, 3492 (1986).
- [57] B. Kendrick and R. T. Pack, Recombination resonances in thermal $H + O_2$ scattering, *Chem. Phys. Lett.* **235**, 291 (1995).
- [58] V. Kokoouline, A. Alijah, and V. Tyuterev, Lifetimes and decay mechanisms of isotopically substituted ozone above the dissociation threshold: Matching quantum and classical dynamics, *Phys. Chem. Chem. Phys.* **26**, 4614 (2024).
- [59] A. Teplukhin and D. Babikov, Several levels of theory for description of isotope effects in ozone: Symmetry effect and mass effect, *J. Phys. Chem. A* **122**, 9177 (2018).
- [60] Z. Darakjian and E. F. Hayes, Extension of the Pack–Parker quantum reactive scattering method to include direct calculation of time delays, *J. Chem. Phys.* **93**, 8793 (1990).
- [61] Z. Darakjian, E. F. Hayes, G. A. Parker, E. A. Butcher, and J. D. Kress, Direct calculation of collisional properties that require energy derivatives of the S-matrix: Results for the reaction $He + H_2^+ \rightleftharpoons HeH^+ + H$, *J. Chem. Phys.* **95**, 2516 (1991).
- [62] Z. Darakjian, E. F. Hayes, G. A. Parker, E. A. Butcher, and J. D. Kress, Erratum: Direct calculation of collisional properties that require energy derivatives of the S-matrix: Results for the reaction $He + H_2^+ \rightarrow HeH^+ + H$ [*J. Chem. Phys.* 95, 2516 (1991)], *J. Chem. Phys.* **101**, 9203 (1994).
- [63] Z. Darakjian, P. Pendergast, and E. F. Hayes, Direct calculation of time delays and eigenlifetimes for the reaction $He + H_2^+ \rightleftharpoons HeH^+ + H$, *J. Chem. Phys.* **102**, 4461 (1995).
- [64] B. R. Johnson, The multichannel log-derivative method for scattering calculations, *J. Comput. Phys.* **13**, 445 (1973).
- [65] D. E. Manolopoulos, An improved log-derivative method for inelastic scattering, *J. Chem. Phys.* **85**, 6425 (1986).
- [66] R. B. Walker and E. F. Hayes, Direct determination of scattering time delays using the R-matrix propagation method, *J. Chem. Phys.* **91**, 4106 (1989).
- [67] G. Guillon and T. Stoecklin, Analytical calculation of the Smith lifetime Q-matrix using a Magnus propagator: Applications to the study of resonances occurring in ultracold inelastic collisions with and without an applied magnetic field, *J. Chem. Phys.* **130**, 144306 (2009).